NOAA Technical Memorandum ERL NHRL-95

U.S. DEPARTMENT OF COMMERCE
NATIONAL OCEANIC AND ATMOSPHERIC ADMINISTRATION
Environmental Research Laboratories

Numerical Experiments of Relevance to Project STORMFURY

STANLEY L. ROSENTHAL
MICHAEL S. MOSS

National
Hurricane
Research
Laboratory
CORAL GABLES,
FLORIDA
December 1971

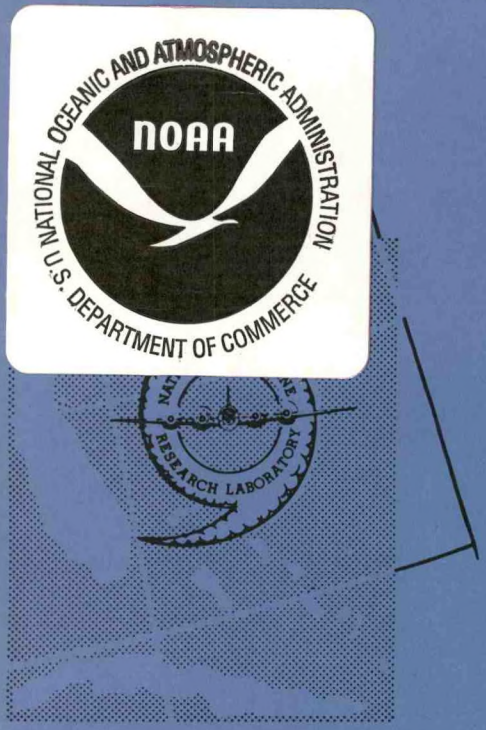

NATIONAL OCEANIC AND ATMOSPHERIC ADMINISTRATION

ENVIRONMENTAL RESEARCH LABORATORIES

NATIONAL HURRICANE RESEARCH LABORATORY TECHNICAL MEMORANDA

Reports by units of the NOAA Environmental Research Laboratories, contractors, and cooperators working on the hurricane problem are preprinted in this series to facilitate immediate distribution of the information among the workers and other interested units. As the limited reproduction and distribution in this form do not constitute formal scientific publication, reference to a paper in the series should identify it as a preprinted report.

Other reports in this series have been prepared by the National Hurricane Research Project of the U.S. Weather Bureau, by the National Hurricane Research Laboratory, as a part of the Weather Bureau Technical Note Series, and as NHRL Technical Memoranda, a subseries of the Institute of Environmental Research Technical Memoranda series.

Beginning with No. 81, they are identified as NHRL Technical Memoranda, a subseries of the ESSA Research Laboratories (ERL). Beginning with No. 90, they are identified as ERL NHRL Technical Memoranda, a subseries of the NOAA Environmental Research Laboratories (ERL).

The reports are available, at a cost of $3.00 per hard copy (microfiche 95 cents), from the National Technical Information Service, Operations Division, Springfield, Virginia 22151.

U.S. DEPARTMENT OF COMMERCE
National Oceanic and Atmospheric Administration
Environmental Research Laboratories

NOAA Technical Memorandum ERL NHRL-95

NUMERICAL EXPERIMENTS OF RELEVANCE TO PROJECT STORMFURY

Stanley L. Rosenthal
Michael S. Moss

National Hurricane Research Laboratory
Coral Gables, Florida
December 1971

TABLE OF CONTENTS

NUMERICAL EXPERIMENTS OF RELEVANCE TO PROJECT STORMFURY

Stanley L. Rosenthal and Michael S. Moss

A number of new experiments which provide theoretical guidance for Project STORMFURY are summarized. The results indicate that artificial heating just radially outward from the eyewall produces the most rapid reduction of the maximum winds at sea level. Older model storms are found to react more rapidly to artificial heating than younger storms. If a substantial reduction of the maximum wind is to be obtained, the artificial heating must be allowed to remain in effect until a new eyewall is formed at a radius greater than that of the original eyewall.

1. INTRODUCTION

This report describes numerical experiments that provide theoretical guidance for Project STORMFURY. The numerical model employed (Rosenthal, 1970a, 1970b, 1971c) is clearly representative of the current state of the art as may be verified by comparison with models developed by Ooyama (1969), Sundqvist (1970) and Yamasaki (1968).[1] It should be made clear, however, that these models are highly idealized theoretical tools. While gross qualitative comparisons can be made with certain aspects of real hurricanes, model results are representative only of some sort of "average" or "typical" hurricane. Skillful prediction from real initial data for a specific hurricane is still a thing of the future.

---

[1]The National Hurricane Research Laboratory has recently developed a hurricane model (Anthes et al., 1971) which eliminates the assumption of circular symmetry and, therefore, is more advanced than those cited in the text.

In addition, a fair amount of uncertainty arises in simulations of hurricane modification experiments since the diabatic effects due to latent heat release are highly parameterized with no explicit representation of the cloud physics.[2] Hence, techniques for representing the seeding of supercooled clouds through silver iodide seeding are quite arbitrary.

Despite these difficulties, it is our opinion that helpful information may be obtained through controlled numerical experimentation. Some preliminary results based on this approach have already been published (Rosenthal, 1971a). Later sections of this paper present a number of new experiments as well as a reassessment of some of the older calculations.

2. REVIEW OF THE MODEL

A brief description of the main features of the model is given below. (The reader concerned with mathematical details should refer to Rosenthal (1970a).) The model storm is an isolated, stationary, circularly symmetric vortex. The vertical structure of the atmosphere is represented by seven levels and geometric height is the vertical coordinate. The levels correspond to pressures of 1015, 900, 700, 500, 300, 200 and 100 mb in the mean tropical atmosphere. All variables are defined at all levels. The primitive equations govern the horizontal motion. The hydrostatic assumption is employed.

---

[2] Estoque (1971) has recently attempted simulations of hurricane seeding experiments with a model incorporating Kessler's cloud physics. Unfortunately, Estoque's equations appear to be more representative of layer clouds than convective clouds.

The continuity equation is simplified as follows. The local rate of change of density is neglected and a climatological density (a function of height alone) is used to evaluate the vertical and horizontal mass flux terms. We then eliminate the external gravity wave by demanding that the vertical integral of the horizontal mass divergence vanish.

In the experiments discussed here, the radial limit of the computational domain is 440 km. The system is open at the lateral boundary. The lateral boundary conditions require that the relative vorticity and horizontal divergence vanish. In addition, the radial derivatives of potential temperature and specific humidity are also required to vanish.

Through a generalization of the procedure suggested by Kuo (1965), the model simulates convective precipitation (and the macroscale heating due to this latent heat release) as well as the enrichment of the macroscale humidity due to the presence of the cumuli. Convection may originate in any layer provided that the layer has a water vapor supply from horizontal convergence and that conditional instability exists for parcels lifted from the layer. Non-convective precipitation is also simulated. Details are given by Rosenthal (1970a).

Time derivatives are estimated by forward differences except in the case of specific humidity where a Matsuno (1966) type integration is employed. Advective derivatives are calculated by the upstream method except for the case of humidity where a conservation form of the equations is used. All nonadvective space derivatives are calculated as centered differences.

The drag coefficient is represented by Deacon's empirical relationship (Roll, 1965, p. 160) which is a linear function of surface-wind speed. The sensible and latent heat fluxes at the sea surface are calculated by the bulk aerodynamic equations and the surface drag is represented by the usual quadratic stress law. The exchange coefficients for sensible and latent heat are equal to the drag coefficient. The turbulent flux convergences that appear in the thermodynamic and water vapor continuity equations are evaluated through the assumption that the fluxes have a linear variation over height and are zero at and above the height of the 900-mb level. This is based on the assumption that at 900 mb and above, fluxes produced by small scale turbulence are insignificant in comparison to those produced by cumulus-scale motions.

The sea temperature is an external parameter and, for experiments discussed here, is taken 2°C greater than the initial sea-level air temperature (initially, the latter is horizontally uniform for all experiments). Since the sea-level air temperature varies with time according to the thermodynamic equation, the air-sea temperature difference varies both with radius and time as the model hurricane evolves.

Radial resolution is 10 km and the time step is 2 minutes. A lateral mixing coefficient of 2.5×10^3 m^2 sec^{-1} is used for all prognostic variables.

3. THE CONTROL EXPERIMENT

The model is initialized with hypothetical data representative of a weak vortex (Rosenthal, 1970a). With judicious choices of static stability, humidity, sea temperature, etc., a hurricane-like vortex ultimately is developed.[3] The structure of the mature storm is, in general, highly realistic.

For the control experiment (Experiment S-35) employed in this report, initial conditions are established as follows. Climatological potential temperatures (a function of height alone and very nearly those of the Hebert and Jordan (1959) mean hurricane season sounding) are specified. With a lower boundary condition of 1015 mb, hydrostatic base-state pressures and temperatures (table 1) are computed for the levels above the surface.

The initial temperature field is then specified by

$$T_{i,j} = \overline{T}_i + T_* \left\{ \text{Cos} \left(\frac{\pi}{\hat{r}} \right) r_j + 1 \right\} \text{Sin} \left(\frac{\pi}{z_7} \right) Z_i$$

where i and j are, respectively, height and radial indices, $\overline{T}_i$ is the standard temperature (table 1), $T_* = 0.16^\circ K$, $\hat{r} = 440$ km, and z_7 is the height (table 1) of level 7. The initial pressure at level 7 is then taken to be the standard value (table 1) and the hydrostatic equation is integrated downward to obtain the remainder of the initial pressure field. Finally, the gradient wind equation is solved for the initial

---

[3] For discussions of the circumstances under which models of this type do not produce hurricanes, see Rosenthal (1971c) and Anthes (1971).

tangential wind while the initial radial and vertical motions are taken to be zero. The initial surface wind reaches a maximum of 7 m sec^{-1} at a radius of 250 km. The central pressure of the vortex is 1013 mb. A base state relative humidity is specified as a function of height (table 2). By use of the data given by table 1, a base state specific humidity is calculated. The initial specific humidity is then assumed horizontally homogeneous and equal to this base state value.

Table 1. Standard values of thermodynamic variables

Level	Height	$\overline{\theta}$	$\overline{T}$	$\overline{p}$
	(m)	(°K)	(°K)	(mb)
1	0	300	301.3	1015.0
2	1054	303	294.1	900.4
3	3187	313	282.6	699.4
4	5898	325	266.5	499.2
5	9697	340	240.8	299.2
6	12423	347	218.9	199.5
7	16621	391	203.1	101.1

Table 2. Initial values of relative humidity at the information levels

Level	Height	Relative Humidity
	(meters)	(percent)
1	0	90
2	1054	90
3	3187	54
4	5898	44
5	9697	30
6	12423	30
7	16621	30

Although Experiment S-35 has been discussed elsewhere (Rosenthal, 1971c), a detailed summary is presented here since we wish to emphasize different points.

Figure 1 summarizes the control's life cycle in terms of central pressure[4] and maximum sea-level wind. The initial conditions are clearly arbitrary and, therefore, the early portions of the integration are not especially significant. In particular, the rather long "organizational"

[4]Pressure is not defined at zero radius because of a horizontal staggering of variables. As a consequence, central pressure values are taken from a grid point 5 km from the storm center at sea-level.

period (168 hours) required for the vortex to begin intensification is easily altered by changing such arbitrary parameters as the scale and/or intensity of the initial vortex, the size of the computational domain and the lateral boundary conditions (Rosenthal, 1971c). The values of some rather poorly defined physical parameters also strongly effect the organizational period (Rosenthal and Koss, 1968; Rosenthal, 1970a; Rosenthal, 1971c).

The rapid intensification of the storm to the mature stage (see 192 to 240 hours, fig. 1) is fairly typical of real hurricanes. Indeed cases exist where deepening of this magnitude has occurred in as little as 12 to 24 hours. The long, quasi-steady, mature stage is fairly typical of hurricanes which remain over the ocean without encountering cold surface waters or unfavorable surrounding flow patterns.

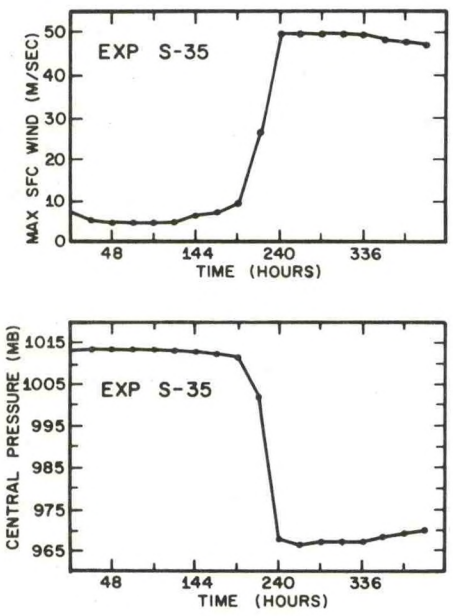

Figure 1. Results from experiment S-35. Top, maximum surface wind as a function of time. Bottom, central pressure as a function of time. Taken from Rosenthal (1971c).

Figures 2, 3, 4, 5 and 6 illustrate structural features fairly representative of the mature stage between 240 and 336 hours. The strongest winds (fig. 2) are concentrated in a narrow zone near the storm center. The strongest vertical motions (fig. 3) and condensation heating as represented by the rainfall rate, (analogous to the hurricane eye wall, fig. 4) are also concentrated in an extremely narrow zone which extends from slightly outside to slightly inside the wind maximum. The radial motions (fig. 5) show that virtually all of the storm's inflow occurs in the lower kilometer of the atmosphere while significant outflow occurs only in the high troposphere. The transverse circulation is then characterized by inflowing air very close to the surface, ascent in the vicinity of the wind maximum and outflow at high levels.

Close to the sea surface, the tangential wind is controlled by the opposing effects of angular momentum conservation as air spirals inward and loss of angular momentum to the ocean through surface drag. This then explains the close association of the eyewall and the wind maximum since it is in the eyewall region that large centrifugal and coriolis effects prevent further inward penetration of the air and hence force ascent to take place. Inflow is concentrated close to the sea surface because the rotational stability of the mature vortex does not allow inward penetration unless absolute angular momentum (following a parcel) is rapidly dissipated (Rosenthal, 1971c) and surface drag provides the only sink sufficient to allow significant penetration. The outflowing branch of the circulation in the high troposphere is largely controlled by conservation of absolute angular momentum since frictional forces are small at these levels.

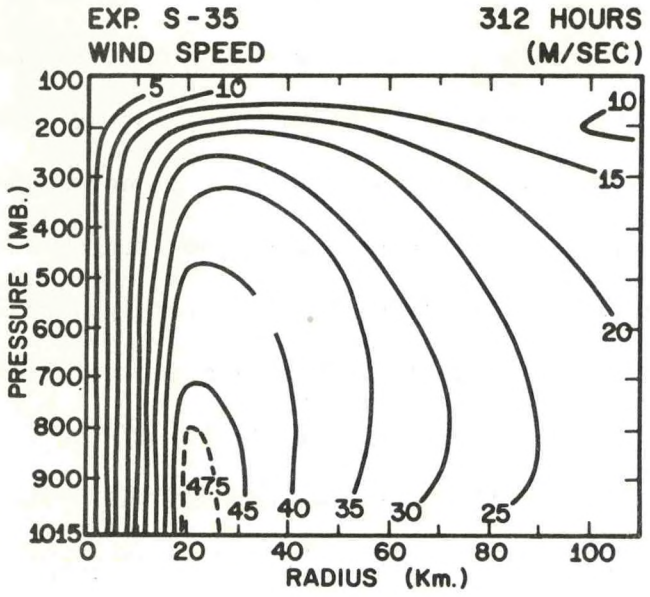

Figure 2. Cross section of wind speed at 312 hours of experiment S-35. Isotachs are labelled in m sec^{-1}. Taken from Rosenthal (1971c).

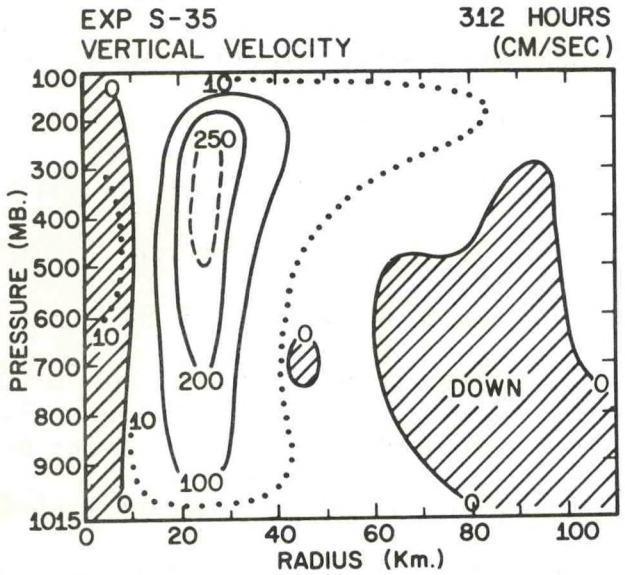

Figure 3. Cross section of vertical velocity at 312 hours of experiment S-35. Isotachs are labelled in cm sec^{-1}. Hatched areas indicate negative values (subsidence). Taken from Rosenthal (1971c).

The fact that the wind maximum (fig. 2) and the isotachs inward of the maximum are essentially vertical is a consequence of the control of the midtropospheric wind field by vertical transports of absolute angular momentum (Rosenthal, 1970b).

The model very nicely provides a subsiding eye (fig. 3) at the storm center. The region of weaker subsidence at larger radii reflects the well known "sucking" effect of rotational boundary layers and has been noted by previous hurricane modelers (Ooyama, 1969). This subsidence is an extremely important feature of the hurricane (Ooyama, 1969; Rosenthal, 1971c). Air parcels entering the inflow layer from midtropospheric levels are relatively dry and have lower equivalent potential temperature than the boundary-layer air. If this air does not gain sufficient water vapor by evaporation from the ocean as it spirals inward, its potential buoyancy upon reaching the eyewall will be small and the cumulus convection required to drive the hurricane will diminish. Numerical experiments (Ooyama, 1969; Rosenthal, 1971c) have verified that model hurricanes rapidly dissipate when oceanic evaporation is suppressed. Observationally, it is well known that cold surface waters suppress hurricane development and lead to filling of existing storms.

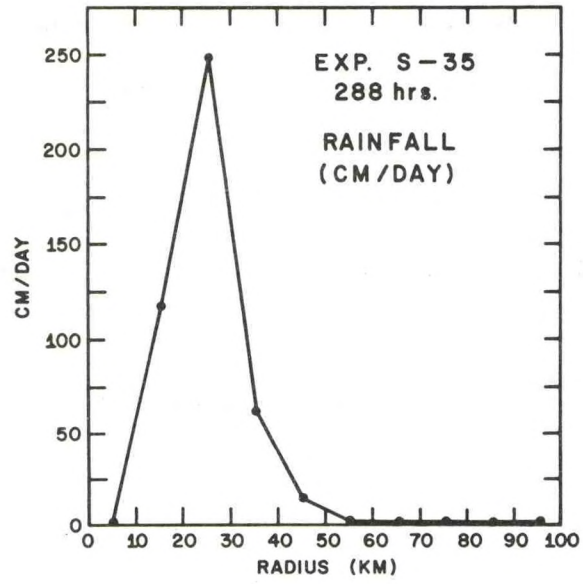

Figure 4. Radial profile of rainfall rates at 288 hours of experiment S-35.

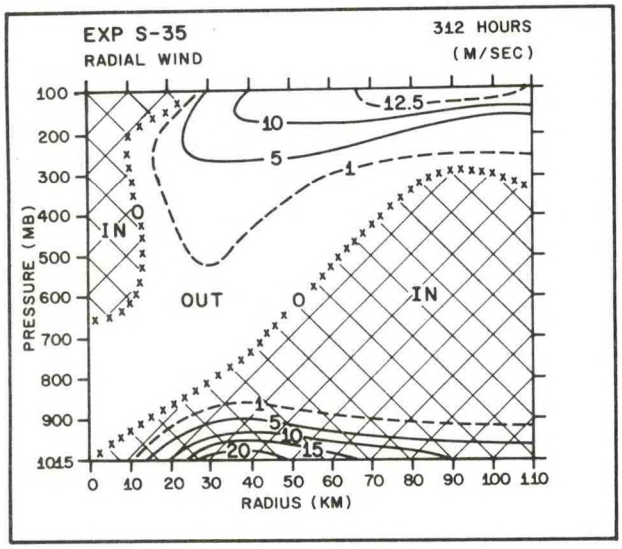

Figure 5. Cross section of radial velocity at 312 hours of experiment S-35. Hatched areas depict inflow.

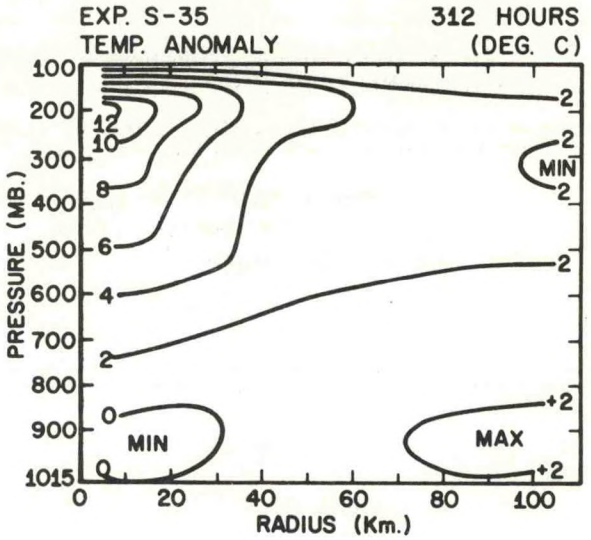

Figure 6. Cross section of temperature anomalies at 312 hours of experiment S-35. Isotherms are labelled in degrees K. Taken from Rosenthal (1971c).

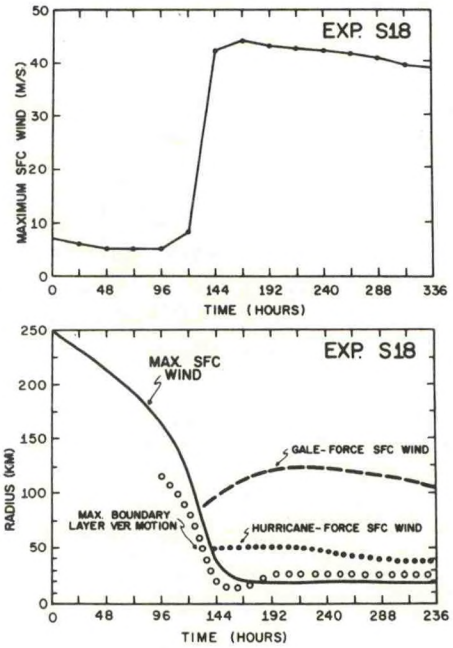

Figure 7. Results from experiment S-18. Top, maximum wind at sea level as a function of time. Bottom, radii of maximum wind at sea level, outer limits of hurricane and gale force winds, radius of maximum 900-mb vertical velocity. Taken from Rosenthal (1971a).

Table 3. Sensible heat flux and evaporation rates for Hurricane Daisy (1958) and experiment S-35 at 312 hours. Rainfall rates for experiment S-35 also shown.

	Average values from model for radial interval 0-100 km at 312 hours	Average values for Hurricane Daisy for radial interval 0-80 n mi on 27 Aug. 1958
Sensible Heat Flux ($cal\text{-}cm^{-2}\text{-}sec^{-1}$)	1.5×10^{-3}	2.9×10^{-3}
Evaporation ($cm\text{-}day^{-1}$)	1.8	2.3
Rainfall ($cm\text{-}day^{-1}$)	22	

Table 4. Kinetic energy generation and dissipation by surface drag friction for Hurricane Daisy (1958) and experiment S-35 at 312 hours.

	Integrated values from model for radial interval 0-100 km at 312 hours	Integrated values for Hurricane Daisy for radial interval 0-60 n mi on 27 Aug. 1958
Kinetic Energy Production (10^{14} $KJ\text{-}day^{-1}$)	5.8	4.6
Kinetic Energy Dissipation by Surface Friction (10^{14} $KJ\text{-}day^{-1}$)	2.9	2.1

Tables 3 and 4 make some comparisons between the mature stage of the model and that of Hurricane Daisy (1958). The data for Hurricane Daisy are taken from Riehl and Malkus (1961). In view of the observational uncertainties in the empirical estimates and the natural storm to storm variability (compare estimates by Riehl and Malkus (1961) with Hawkins and Rubsam (1968) and Miller (1962)), the agreement between the model values and those for Hurricane Daisy is certainly satisfactory.

4. SUGGESTED TACTICS FOR HURRICANE MODIFICATION

What we will refer to as "Hypothesis I" was first put forth by Simpson et al. (1963) and later published in more polished form by Simpson and Malkus (1964). Simpson and Malkus recognized that the hurricane wall cloud is located quite close to the region of maximum low-level pressure gradient and further contended that the wall cloud contains significant quantities of supercooled water. According to the hypothesis, if this supercooled water were frozen through nucleation by silver iodide crystals, the released heat of fusion would produce temperature increases; and therefore, hydrostatically, pressure decreases near the region of the strongest pressure gradient. If the central pressure did not concomitantly decrease, a reduction in maximum pressure gradient and, in turn, a reduction in wind speed should be the net result. Temperature increases of 2°C were estimated on the assumption of freezing 1 gm m^{-3} of supercooled water in the layer 500 to 150 mb. With the further assumption that the 150-mb surface remains unaltered, hydrostatic arguments were invoked to estimate reductions at the seeded radii of as much as 200 ft

in the heights of the pressure surfaces at and below 500 mb. This, in turn, was expected to reduce the maximum pressure gradient force by 10 to 15 percent.

Questions which are difficult to answer can be raised concerning both the actual supercooled liquid water content of eyewall clouds and the efficiency of the seeding operation in freezing this supercooled water (see Section 5 and Gentry and Hawkins, 1971). However, Hypothesis I is also questionable from other points of view. The estimates of temperature increase to be realized from the released heat of fusion assume a constant pressure process. It is, however, not unlikely that the air would follow an ice pseudoadiabat with substantial amounts of the heat of fusion being converted to potential rather than internal energy.

An even more critical consideration is the fact that the eyewall drives the storm's transverse circulation and seeding this region alone would very likely accelerate this circulation thus providing a more rapid inflow of both angular momentum and water vapor to the eyewall region.

Diagnosis of the results of a number of numerical experiments led to a proposed strategy which is a slight tactical variant of Hypothesis I (Rosenthal, 1971a). Typically, the organizational period for a developing model storm does not terminate until a concentrated vertical-velocity maximum (eyewall) develops at a radius smaller than that of the low tropospheric wind maximum. Once this feature appears, the storm deepens rapidly and, at the same time, the eyewall and wind maximum migrate inward. The wind maximum, however, moves more rapidly than the eyewall. Invariably development ceases when the eyewall and wind maximum become

nearly coincident. (An example taken from a previous paper is shown by fig. 7.) The sequence is clearly consistent with the angular momentum considerations of the previous section.

Hypothesis II differs from Hypothesis I in that the latter calls for seeding the eyewall alone whereas the former suggests seeding either from the eyewall outward or entirely outward from the eyewall. While the logistics of these hypotheses differ only slightly, the physical arguments are substantially different. In Hypothesis II, the basic idea is to stimulate convection and ascent at radii greater than that of the eyewall. The region of stimulated convection is intended to compete with the eyewall for the inflowing air at low levels. If significant portions of the inflow can be diverted upward at the seeded radii, the angular momentum and water vapor supplies to the original eyewall and wind maximum will be reduced. As a consequence, one would expect the original wind maximum to be reduced and the eyewall convection to be diminished.[5]

5. PROCEDURES FOR THE SEEDING SIMULATIONS

Since the hurricane model contains no cloud physics, simulation of silver-iodide seeding through the application of basic physical laws, as has been done in cloud models (e.g. Cotton, 1970), is not yet possible. The techniques employed are, therefore, highly pragmatic and presuppose the occurrence of certain cloud physical processes. They have evolved from extensive discussion with those involved in the field program

[5]A similar proposal has been put forth by Sundqvist (1970). He, however, suggested seeding experiments at extremely large radii.

(Gentry, 1969; Gentry and Hawkins, 1971; Rosenthal, 1971a). An early and extremely crude version of the model (Rosenthal, 1969) was used in 1968 to simulate seeding of the hurricane by silver iodide. These calculations were intended to simulate "single seeding" field experiments in which the seeder aircraft discharges its material once in a pass of 2-3 min covering a radial interval of about 30 km. The feeling of those involved in the field program (Gentry, 1969) was that a single-seeding experiment could release heat of fusion over the 500- to 300-mb layer equivalent to a heating rate of 2°C/30 min and lasting for a period of 30 min. At 300 mb, this amounts to freezing about 2.5 g water$\cdot m^{-3} \cdot (30\ min)^{-1}$. At 500 mb, the figure is approximately 4 g water$\cdot m^{-3} \cdot (30\ min)^{-1}$. While the release of silver iodide is made along a particular azimuth, those involved in the field program felt that the circulation of the storm sweeps the material in a more or less circular path, thus providing the heating rates cited above in a circular fashion. To simulate this process, the heating function that represents the cumulus feedback on the macroscale (Rosenthal, 1969) was simply increased by the amount and for the period cited above at selected radii.

By August 1969, the design of the field experiment (Gentry, 1970) had been altered such that single seedings (as previously defined) were repeated five times at 2-hr intervals. Since the model had been substantially improved by this time and since no simulations of multiple-seeding experiments had as yet been carried out, a new series of calculations (Rosenthal, 1971a) were performed. The heating rates for these seeding simulations were established after discussion with Dr. Gentry (NHRL).

These consultations revealed that he continued in his belief that 2°C/30 min was the correct heating rate for a single seeding. However, he was now of the opinion that the effect would be felt for at least 1 hr (in contrast to the 0.5 hr cited at the time of the 1968 calculations). It was also Dr. Gentry's feeling that the enhanced heating might be more or less continuous over the 10-hr period spanned by the multiple-seeding operation.

The heating functions were enhanced at 300 and 500 mb which are the model levels corresponding to the layer seeded in the field experiment. Calculations were performed where the enhanced heating was applied continuously for ten hours and intermittently at 2-hr intervals for 30 minutes. Differences between calculations with continuous and intermittent enhanced heating were relatively minor. Consequently, because of conceptual simplicity, the continuous heating was adopted as a basic procedure.

Generally speaking, the earlier calculations (Rosenthal, 1971a) favored Hypothesis II over Hypothesis I. They also appeared to provide a response time to the simulated seeding which compared favorably to that observed in the Hurricane Debbie (1969) field experiment (Gentry, 1970; Hawkins, 1971) if one assumes the changes in Debbie were indeed produced by the seeding. As we will see later, this may have been a fortuitous result produced by choice of initial conditions. Unfortunately, this was not suspected during 1969 and 1970 when extensive empirical investigations pertinent to hurricane seeding were under progress at NHRL.

In the meantime, new studies of cloud-physics data obtained in unseeded hurricanes (Sheets, 1969; Gentry and Hawkins, 1971) led to the tentative conclusion that the supercooled water content of the major eyewall clouds was similar to that already suggested by Simpson et al. (1963) and Gentry (1969). At this time, however, Gentry and Hawkins (1971) did a more careful analysis of the rate of release of heat of fusion which might be expected under optimal field conditions. For such a calculation, the supercooled water content of clouds is only one of the important parameters. Other crucial factors include, at the very least; (1) the time scale for freezing supercooled water by silver-iodide nucleation, (2) the time scale over which silver iodide is active and effective as freezing nuclei in a given cloud updraft, (3) the time scale for the regeneration of an equivalent amount of supercooled water in the updraft, (4) the effectiveness and time scale of nucleation of supercooled water by the ice crystals formed from the silver-iodide seeding, (5) the number of clouds available for seeding, (6) the number of clouds which reasonably can be expected to be seeded by a field operation of the type previously described.

Observational data for establishing all of these parameters in the hurricane context do not exist. Gentry and Hawkins (1971) made the reasonable (and implicit) assumption that time scales (1) and (2) were on the order of 1-2 minutes while time scale (3) was much larger. (Simple calculations on a pseudoadiabatic chart indicate time scale (3) to be 500 to 1000 secs for a 5 m sec^{-1} updraft.) With these assumptions for time scales (1), (2) and (3) and with 100 percent freezing efficiency, we

deduce a pulse-like heating function (in a cloud) 15 to 30 times the normal heating rate used in the previous simulations (Rosenthal, 1971a) but existing only for a few minutes. In view of time scale (3), substantial freezing by ice nucleation of newly generated supercooled water does not appear likely. If we average the heating pulse over two hours (the time between seedings) we obtain a heating function per seeded eyewall cloud of .25 to .50 of the normal rate used in the simulations.

However, we must also take into account that the heating functions applied to the model are averages over 10 km (distance between grid points) of radial distance and 360 degrees of azimuth angle. In view of the fact that even in the eyewall the areal coverage of active updrafts is less than 10% (Malkus, 1960) and that the areal coverage decreases rapidly with radius and considering the rate of azimuthal transport of silver iodide by the tangential wind, Gentry and Hawkins (1971) concluded that the rate of release of heat of fusion in Hurricane Debbie was probably 1 to 2 orders of magnitude less than the normal rate used for the model simulations.

As a consequence, the authors were asked to conduct calculations under Hypothesis II with successively smaller heating until a ten hour operation failed to provide responses similar to those obtained previously. The first of these calculations was made with half the normal rate and already showed no significant response. (At this time, we were still not aware of the dependence of model response on initial conditions.)

Soon after this, however, a new and highly attractive view of the cloud-physical response to silver-iodide seeding emerged. The members of

the Project STORMFURY Advisory Panel (1971) wrote, "The augmented heating rates used to simulate seeding probably cannot be realized in nature solely from release of latent heat of fusion. The most reasonable analog in nature is the possibility that convective clouds in the region just outside the existing eyewall could be stimulated by seeding to more active growth and intensity thus replacing the previous eyewall with a new one at a greater radius. Augmented heating from enhanced condensation, plus freezing in such circumstances, probably exceeds the augmented heating rates used in the seeding simulations."

The macroscale dynamical aspects are here identical to Hypothesis II in that the strategy is to divert inflowing air to rise at radii greater than that of the eyewall. The field tactics are also identical and call for seeding radially outward from the eyewall. In addition to the augmented heating expected under this approach, there is an interesting and beneficial side affect. Radar data (Senn, 1971) indicate that more than 50 percent of the cumuli within 30 nm of the hurricane center have tops within the 20,000- to 30,000-ft range. Since, in most hurricanes, very little macroscale inflow or outflow occurs at middle tropospheric levels (Riehl and Malkus, 1961; Miller, 1962; Hawkins and Rubsam, 1968), the mass transported upward in clouds whose tops are at these levels must subside relatively close to the cloud and thus reduce the net upward mass transport. If through silver-iodide seeding these clouds can be induced to grow vertically into the outflow layer not only would the additional latent heat postulated by the STORMFURY Advisory Panel be realized but also, the mass transported upward would be caught in the macroscale

outflow and evacuated from the storm core. Consequently, this so-called "New Hypothesis" provides not only a larger heat source but also a more efficient mechanism for evacuating the air diverted from the inflow layer.[6] Calculations by Sheets (1969) indicate that individual clouds just beyond the eyewall can be induced to grow to outflow levels by silver-iodide seeding.

While the postulated mechanisms of the new hypothesis appear capable of providing heat at rates which approach the values used in the model calculations (see also Gentry and Hawkins, 1971), some conceptual problems arise with the model simulations. The major source of energy is now to be obtained from clouds which are induced to grow from mid- to upper-tropospheric levels. However, the model parameterization of cumulus activity is essentially a generalization of the technique introduced by Kuo (1965) in which model clouds are comprised of undilute ascent. Consequently, all model clouds whose bases are in the boundary layer reach upper tropospheric levels by natural processes. The model eyewall differs from other regions of the storm in cloud concentration but not in cloud depth. This is a distinct discrepancy between model and real hurricanes (Senn, 1971; Malkus, 1960).

Simulations relevant to the new hypothesis are not easily visualized unless one adopts a highly philosophical attitude. The basic feature, it may be argued, is the stimulation of tall convection at radii beyond the

[6]Despite differences between hypotheses, all flight tracks for hurricanes seeded to date have been more or less the same (Gentry and Hawkins, 1971).

eyewall. In the field program, this is to be accomplished by causing relatively short clouds to become tall. The ultimate effect, however, is to increase the concentration of tall clouds in the seeded region. While the current version of the model cannot simulate the intermediate stages in which short clouds grow to tall clouds, the techniques previously employed (Rosenthal, 1971a) do indeed provide for increased tall cloud concentrations in the "seeded" regions.

Consequently, we have retained the original technique for seeding simulation. Aside from the virtue of simplicity, this also allows direct comparisons between the new calculations and those previously published. The technique consists simply of increasing the heating function that represents the cumulus feedback on the macroscale by fixed amounts for certain periods of time. This artificial enhancement of the heating functions is always applied at only the 300- and 500-mb levels.[7] The radial interval and duration of seeding varies from experiment to experiment and is clearly stated in each case. The "normal" enhancement rate is retained as the equivalent of a 2°C per 30 min temperature change at constant pressure (Rosenthal, 1971a). In the meter-ton-second system of units employed in the model, this is approximately 1 kilojoule per ton per second (approximately 4.2×10^{-3} calories per gram per second). For the reader's convenience, the Appendix provides a table which summarizes the essential features of new experiments not discussed in previous publications.

---

[7]For ease of expression, artificial enhancement of the heating function will be referred to as "seeding". We fully realize the looseness of this expression.

6. CALCULATIONS RELEVANT TO HYPOTHESIS I

A previous calculation in which the normal enhanced heating rate was applied for ten hours at the eyewall center (25-km radius) and the next grid point inward (15 km) resulted in a slight intensification of the model storm (see fig. 8, taken from Rosenthal, 1971a) with a rapid recovery to a state close to the control after the seeding was terminated. Examination of the 900-mb vertical motions (fig. 9) clearly showed that boundary-layer convergence was increased at the seeded radii but rather little at other radii.

Two new calculations provide somewhat similar results. The initial data are hour 288 of Experiment S-35. To exaggerate the effect, enhanced heating is applied at twice the normal rate (2 KJ Ton^{-1} sec^{-1}) for 20 hours at 15 and 25 km (Experiment N-12) and 25-km radius (see figs. 3 and 4 for radius of maximum vertical motion). The behavior of maximum sea-level wind (MSLW) for these experiments, summarized by figure 10, is much the same as that obtained from the previous experiment. No further experiments relevant to Hypothesis I have been conducted.

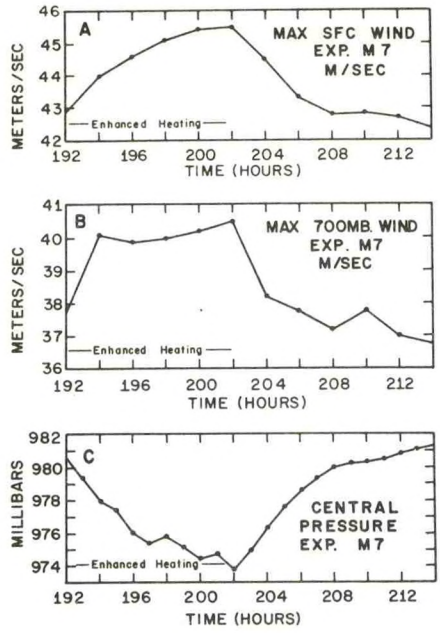

Figure 8. Results from an experiment with seeding at radii of 15 and 25 km from 192 to 202 hours. The rate of artificial seeding is 1 KJ ton^{-1} sec^{-1}. The eyewall is at 25-km radius. The control is experiment S-18 (fig. 7) and is very nearly in steady state during the interval shown. Taken from Rosenthal (1971a).

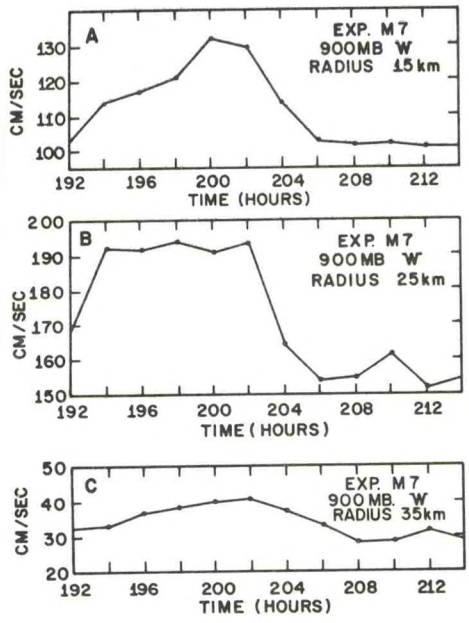

Figure 9. Vertical motions at 900 mb during and after the seeding operation shown by figure 8. Seeding is at radius of 15 and 25 km.

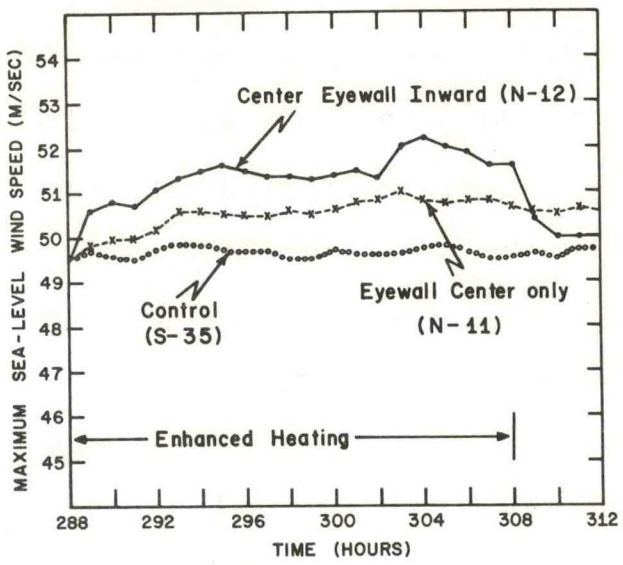

Figure 10. Results from two seeding experiments. Artificial heating is applied from 288 to 308 hours. The initial conditions are hour 288 of experiment S-35. The rate of artificial heating is 2 KJ ton^{-1} sec^{-1}. The eyewall is at 25-km radius. For experiment N-11, artificial heating is applied at 25-km radius. For experiment N-12, artificial heating is applied at 15- and 25-km radius.

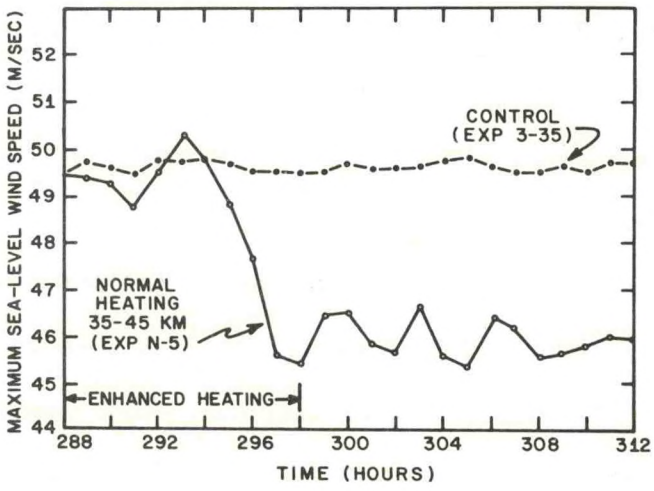

Figure 11. Results from a seeding experiment (N-5) where artificial heating is applied from 288 to 298 hours at radii of 35, 45 and 55 km. The initial conditions are hour 288 of experiment S-35. The eyewall is at 25-km radius.

7. CALCULATIONS RELEVANT TO HYPOTHESIS II

Figure 11 summarizes an experiment (N-5) in which the normal (1 KJ ton^{-1} sec^{-1}) enhanced heating rate was applied for ten hours over a 30 km radial interval just beyond the eyewall center (35, 45 and 55 km). Initial conditions are again 288 hours of S-35. Figures 12 and 13 vividly portray the diversion of boundary-layer inflow and the formation of a new eyewall 10 km radially outward from the original. When the seeding is terminated, the system attempts to restore the original eyewall. Significant changes in MSLW do not occur until the new eyewall has become established which is about eight hours after the start of seeding. Important changes in the wind profile (fig. 14) occur earlier. In response to the increased transverse circulation that is produced by the seeding, angular momentum is carried inward more rapidly than is the case for the control. Consequently, low-level winds increase at all radii larger than that of the MSLW. A later experiment will verify that the increased centrifugal and coriolis forces associated with these low-level wind increases play a vital role in cutting off the supplies of mass and angular momentum to the original eyewall.

Winds at 700 mb (fig. 15) behave quantitatively in a fashion similar to those at sea level. Here, however, the response to seeding is more rapid and extreme. Peak winds exceed those of the control until after seeding is terminated. The rapid response of 700-mb winds in the seeded zone results from lack of the moderating effects of drag friction as well as the increased vertical advection associated with increased vertical

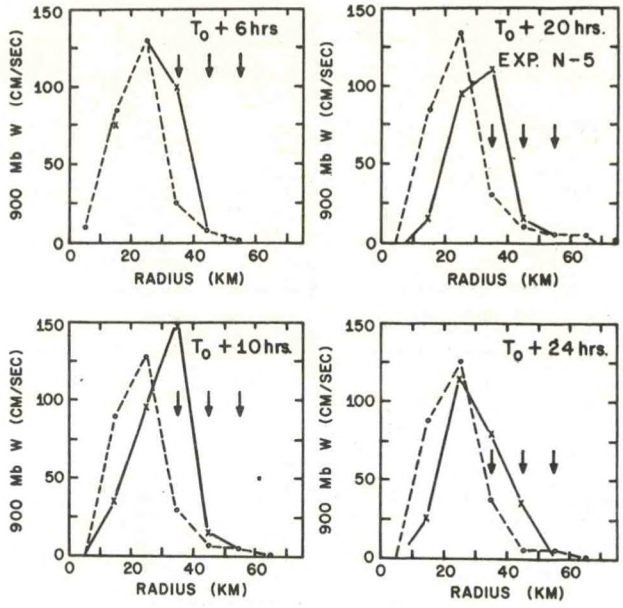

Figure 12. Radial profiles of 900-mb vertical motion at selected times during experiment N-5. The control (S-35) data are shown by dashed lines. The arrows indicate the seeded radii. Initial conditions (T_0) are hour 288 of experiment S-35. Seeding terminates at T_0 + 10 hours.

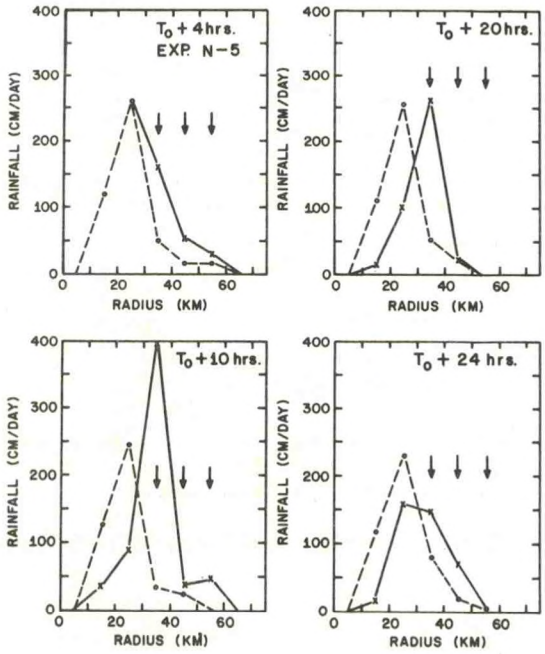

Figure 13. Same as figure 11 but rainfall rates are shown.

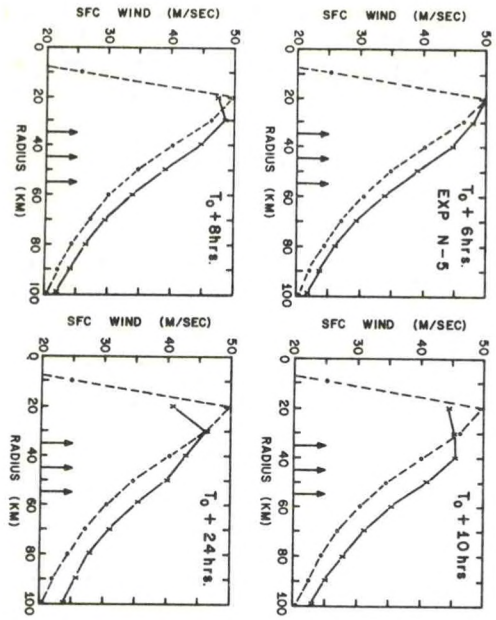

Figure 14. Same as figure 11 but wind speed profiles at sea level are shown.

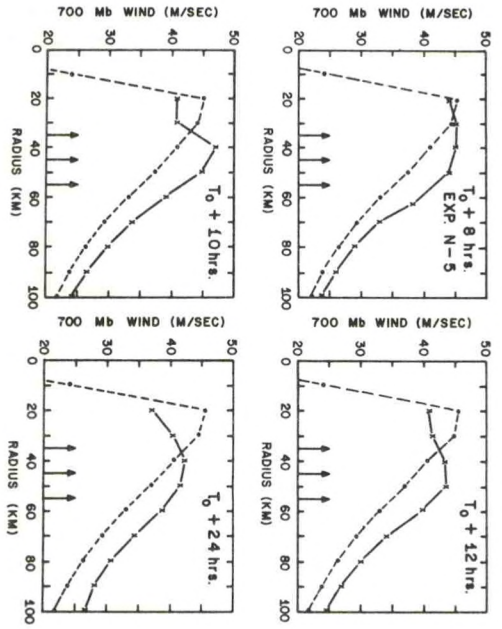

Figure 15. Same as figure 11 but 700-mb wind speed profiles are shown.

motions. These 700-mb results are similar to those previously obtained (Rosenthal, 1971a) and have raised some concern. This stems from the fact that Hurricane Debbie was monitored near 700 mb and showed wind variations more nearly like the model results at sea level. It is the authors' opinion that little information can be drawn from these differences because of the idealized nature of the model. As pointed out earlier, computational results can only validly be compared in detail with other computational results.

The central pressure in Experiment N-5 (not shown) drops 4 mb during the first 8 hours of seeding. As soon as the new eyewall is formed, the central pressure rises and approaches that of the control.

Previous calculations (Rosenthal, 1971a) found only minor differences between experiments in which the seeding was conducted entirely beyond the original eyewall (such as N-5) and those in which seeding was conducted from the original eyewall outward. This appears to be a result of fortuitous initial conditions and not in general true. Experiment N-4 (fig. 16) is identical to N-5 with the sole exception that the seeding is performed at radii of 25, 35 and 45 km and, hence, includes the eyewall center. The MSLW exceeds that of the control during the entire calculation. The behavior of the winds at 700 mb (not shown) is similar to that of the surface winds. The vertical-motion and precipitation patterns (also not shown) show only minor increases at the seeded radii with no tendency for outward displacement of the eyewall.

If, however, the seeding is extended for another ten hours (Experiment N-4D), the ultimate effect is similar to that obtained in N-5

(compare figs. 11 and 16). Thus seeding from the eyewall center outward appears to be a potentially successful tactic but a less desirable one than seeding that entirely avoids the eyewall center.

The major difference in the results of Experiments N-4 and N-4D is that in the former case seeding is terminated just before any important diversions of boundary-layer inflow take place. We are, therefore, left with an increased transverse circulation that is more or less congruent with that of the control. When the seeding is extended in time (Experiment N-4D), the heating beyond the eyewall ultimately becomes effective in stimulating convection and significant diversions of inflow are noted at 300 hours (fig. 17). By 302 hours, the new eyewall is established. Decreases in MSLW do not become significant until 300 hours when the diversion of inflow first becomes apparent.

Two additional experiments, with tactics between those of N-4 and N-4D, yielded interesting results. One of these (N-45) continued seeding just two hours longer than N-4, that is from 288-300 hours. The result, of course, is identical to N-4D until 300 hours. Thereafter, the model storm quickly adjusted in structure and intensity to a state nearly identical to that of N-4. This again indicates that seeding must be continued at least until a new eyewall is established if reductions in MSLW are to be achieved. To further examine this point, the seeding was continued for still another two hours and terminated at 302 hours (N-46). Since this experiment is identical to N-4D from 288 to 302 hours, the eyewall (fig. 17) has already reformed at a radius of 35 km when the seeding is terminated. The result of this experiment (N-46) was very similar to

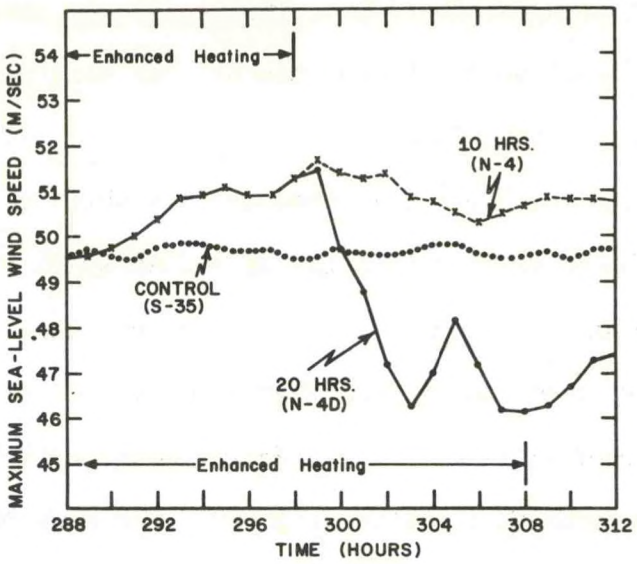

Figure 16. Results from two seeding experiments. The initial conditions are hour 288 of experiment S-35. The artificial heating rate is 1 KJ ton^{-1} sec^{-1} and is applied at radii of 25, 35 and 45 km. For experiment N-4, artificial heating is in effect from 288 to 298 hours. For experiment N-4D, artificial heating is in effect from 288 to 308 hours.

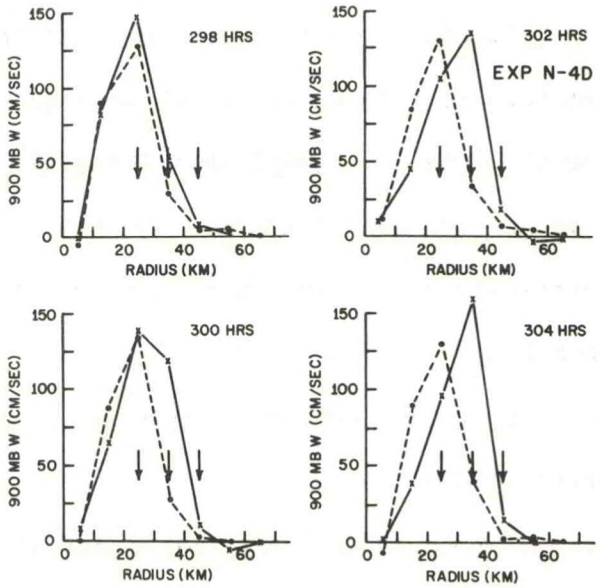

Figure 17. Radial profiles of 900-mb vertical motion at selected times during experiment N-4D. The control (S-35) data are shown by dashed lines. The arrows indicate seeded radii. Initial conditions are hour 288 of experiment S-35. Seeding terminates at 308 hours.

that of N-4D. It appears, therefore, that continued seeding at the same radii after the formation of the new eyewall has no significant effect in further reductions of the MSLW.

An experiment (N-21) was then conducted in which at hour 304 of N-4D the seeded radii were shifted from 25, 35 and 45 km to 35, 45 and 55 km. The heating rate was the normal value and the operation was continued for 16 hours. No consistent deviations from N-4D were observed. An eyewall temporarily appeared at 45-km radius after 6 hours (310 hours) but within two more hours receded to a radius of 35 km. The MSLW for this experiment oscillated around that of N-4D. At 310 hours, when the eyewall was at 45 km, the MSLW was 2.5 m sec^{-1} less than that of N-4D. But by 312 hours, the MSLW was only 1 m sec^{-1} less than that of N-4D. Earlier, at 305 hours, N-21 showed MSLW 1 m sec^{-1} greater than N-4D.

Experiment N-6 (fig. 18) was conducted to determine if increased seeding rates would lead to more rapid responses and/or greater decrease in MSLW. It is identical to N-4 except that the artificial heating is twice (2 KJ ton^{-1} sec^{-1}) the normal value. The response here is much more rapid. The vertical-motion and precipitation patterns (not shown) indicate a new eyewall at 35-km radius by 294 hours. However, despite the more rapid response, the reduction in MSLW is not significantly greater than that observed in N-4D.

In our discussion of Experiment N-5, we stated that an important factor in the formation of a new eyewall at a larger radius is an increase of wind at radii from the seeded zone outward (figs. 14 and 15) during the early portions of the operation. Experimental results in

support of this contention have been deferred to this point. Experiment N-15 (fig. 19) was identical to N-4D with the sole exception that the coriolis and centrifugal terms in the radial equation of motion were held constant at the value given by the initial conditions. The MSLW oscillates about the control (S-35) with no consistent departure. The storm structure yielded by N-15 (not shown) shows no significant differences from S-35. There is absolutely no tendency to form a new eyewall. Therefore, by comparison of N-4D and N-15, we conclude that increased coriolis and centrifugal forces at larger radii are vital if the inflow is to be prevented from reaching the original eyewall and if a new eyewall is to be formed at a larger radius.

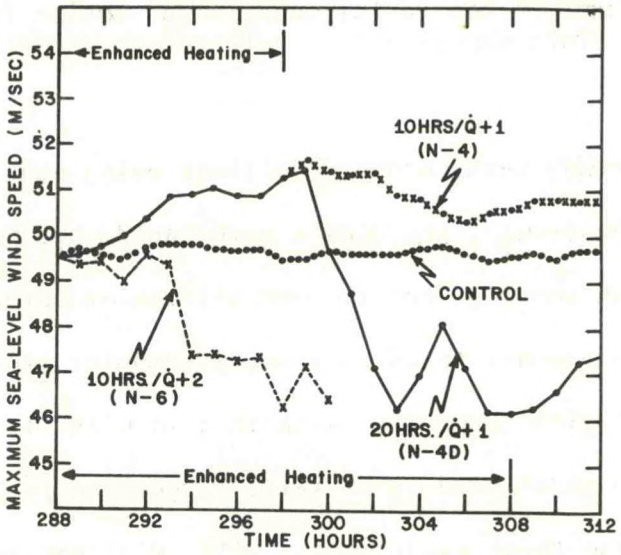

Figure 18. Results from three seeding experiments. The initial conditions are hour 288 of experiment S-35. For experiment N-6, the artificial heating rate is 2 KJ ton^{-1} sec^{-1}. For experiments N-4 and N-4D, the rate is 1 KJ ton^{-1} sec^{-1}. Artificial heating is in effect from 288 to 298 hours in experiments N-6 and N-4. For experiment N-4D, the artificial heating is in effect until 308 hours. The seeded radii are 25, 35 and 45 km for all three experiments.

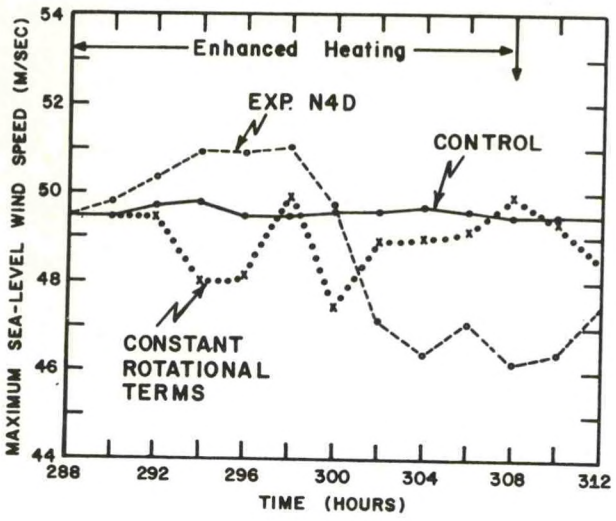

Figure 19. Results from two seeding experiments. The initial conditions are hour 288 of experiment S-35. The artificial heating rate is 1 KJ ton^{-1} sec^{-1} and is applied at radii of 25, 35 and 45 km and is in effect from 288 to 308 hours. The experiment labeled "constant rotational terms" evaluates the coriolis and centrifugal terms in the radial equation of motion from the initial winds. This experiment is referred to as N-15 in the text and appendix.

We have already seen, other conditions being equal, that seeding entirely beyond the eyewall produces a more rapid, but no greater, reduction in MSLW than seeding from the eyewall center outward. In both cases, however, the new eyewall forms only one grid point (10 km) radially outward from the original eyewall. With this in mind, it is of interest to compare the results of seeding at still larger radii. The following questions motivate these experiments: (1) Will the reduction of MSLW occur even more rapidly as the artificial heating is applied at even larger radii? (2) Can larger reductions in MSLW be achieved by seeding at still larger radii? (3) Can we induce eyewall formation with the model at larger radii than observed in the experiments already discussed?

Experiments N-4F, N-13 and N-27 are addressed to these questions. The common aspects of these experiments are the normal heating rate (1 KJ ton^{-1} sec^{-1}) for 20 hours with 288 hours of S-35 constituting the initial conditions. The radial intervals seeded are: 35, 45 and 55 km (N-4F); 45, 55 and 65 km (N-13); 75, 85 and 95 km (N-27). Note that the first 10 hours of N-4F are identical to N-5. Figure 20 gives the MSLW histories for these calculations. The ultimate results of the three experiments are much the same. Furthermore, the variation in response time is opposite in sense from what might have been expected from the results of N-5 and N-4D. It thus appears that the answers to questions (1) and (2) of the previous paragraph are no. The structural evolution of N-13, though lagging in time, is similar to that of N-4F which in turn is similar to N-5 (figs. 12 to 15). In each case, the new eyewall is formed at a radius of 35 km.

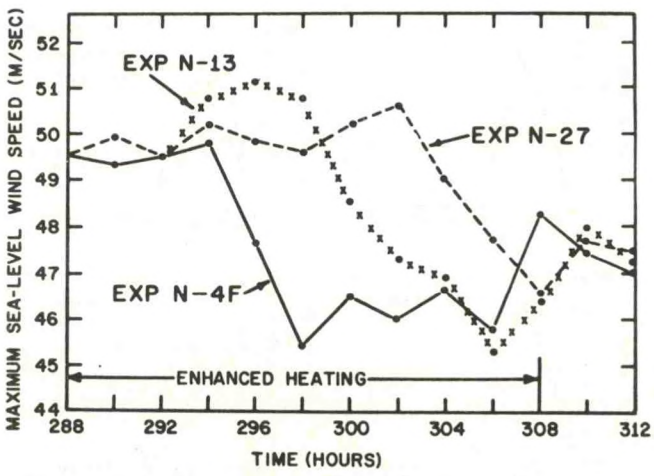

Figure 20. Results from three seeding experiments. The initial conditions are hour 288 of experiment S-35. The artificial heating rate is 1 KJ ton^{-1} sec^{-1} and is in effect from 288 to 308 hours. The seeded radii are: 35, 45 and 55 km (Experiment N-4F); 45, 55 and 65 km (Experiment N-13); 75, 85 and 95 km (Experiment N-27).

Even in experiment N-27, where the seeded zone is 75, 85 and 95 km, the new eyewall is formed at a radius of 35 km. In this case, however, there are some interesting differences in the structural evolution (figs. 21 and 22). At 296 hours, 8 hours after the start of seeding, the only significant response of the 900-mb vertical motions (fig. 21) is a small increase centered at the inner edge of the seeded zone. Between 302 and 304 hours (14 to 16 hours after the start of seeding) significant increases of vertical motion (in comparison to the control) begin to occur at a radius of 35 km. It is at this time that the MSLW (fig. 20) begins to fall. It is not until 308 hours (a full 20 hours after the start of seeding) that the eyewall becomes established at the larger radius. It is also at this time that the MSLW reaches its minimum value (fig. 20). It is interesting that the 900-mb vertical motions at 308 hours in the seeded zone are downward (fig. 21).

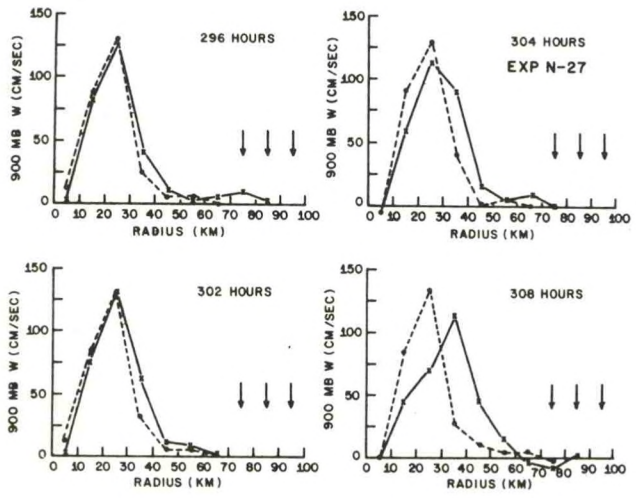

Figure 21. Radial profiles of 900-mb vertical motion at selected times during experiment N-27. The control (S-35) data are shown by dashed lines. The arrows indicate seeded radii. Initial conditions are hour 288 of S-35. Seeding terminates at 308 hours.

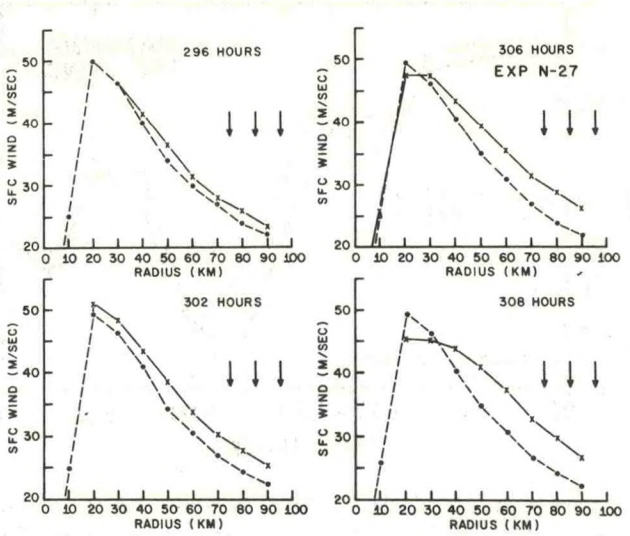

Figure 22. Same as figure 21 except that profiles of sea-level wind speed are shown.

The wind structure at sea level (fig. 22) also shows some differences from the experiments already discussed. In particular, the reduction of MSLW is accomplished without radial displacement. Here, essetially, we observe a flattening of the original sharp maximum and the formation of a plateau-like wind profile with a poorly delineated maximum.

The results thus far show one major discrepancy in comparison to those presented earlier (Rosenthal, 1971a). Experiments with the normal seeding rate applied at radii of 25, 35 and 45 km (Experiments N-4 and N-4D) show a substantially longer response time than those with the same heating rate at radii of 35, 45 and 55 km (Experiments N-5 and N-4F). Similar experiments summarized by Rosenthal (1971a) did not show this difference as may be verified by examination of figure 23.

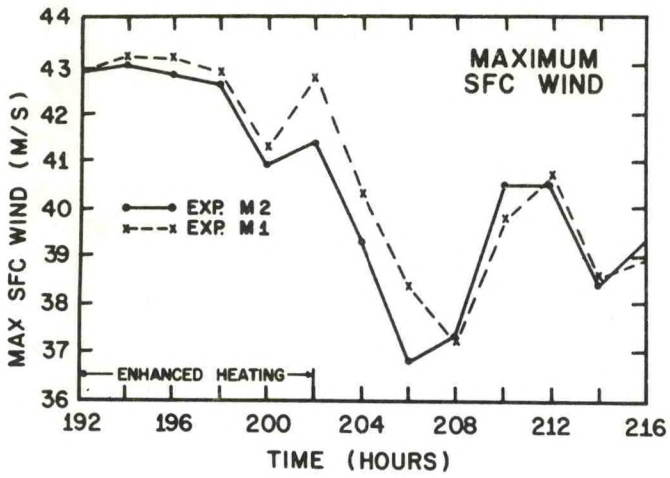

Figure 23. Results from two seeding experiments. The rate of artificial heating is 1 KJ ton^{-1} sec^{-1} and is in effect from 192 to 202 hours. The control is very nearly in steady state during the interval shown and has its eyewall at 25-km radius. In experiment M-1, seeding is at radii of 25, 35 and 45 km. For experiment M-2, the seeding is at radii of 35, 45 and 55 km. Taken from Rosenthal (1971a).

It was originally thought that this discrepancy was attributable to a change in the treatment of the drag coefficient[8] introduced in the interim between the two sets of calculations. However, the calculations discussed below indicate that a more likely explanation may be found in differences in initial conditions.

Figure 24 summarizes departures from the control MSLW obtained from four experiments with the normal heating rate applied for 20 hours at 25, 35 and 45 km. The initial conditions for these experiments are the control (S-35) at 264 hours (N-22), 288 hours (N-4D), 312 hours (N-23) and

[8]A constant drag coefficient of 3×10^{-3} was used in the old calculations. The present calculations use a drag coefficient which is a linear function of wind speed. See Rosenthal (1971c) for details.

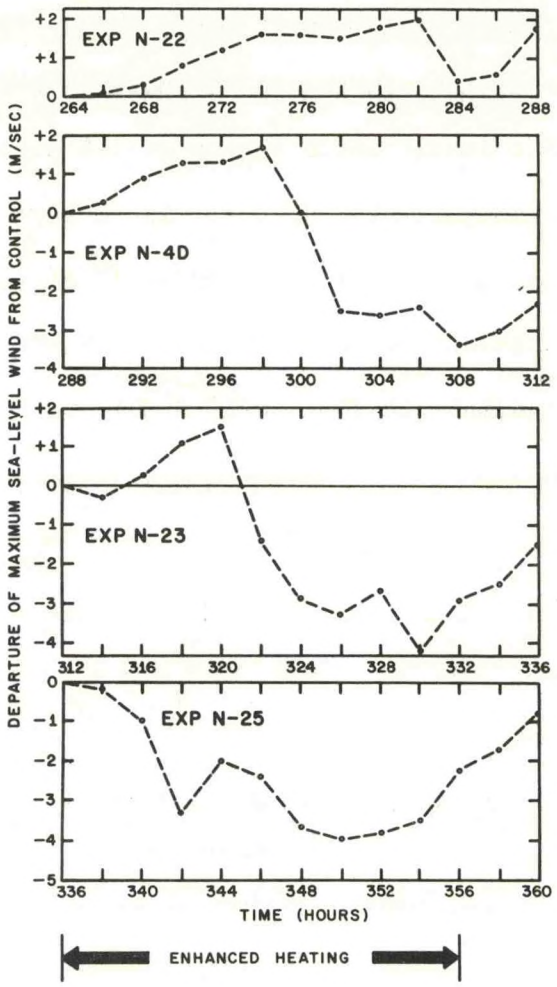

Figure 24. Results from four seeding experiments. The rate of artificial heating is 1 KJ ton^{-1} sec^{-1} and is in effect for 20 hours at radii of 25, 35 and 45 km. The initial conditions are: hour 264 of S-35 (Experiment N-22); hour 288 of S-35 (Experiment N-4D); hour 312 of S-35 (Experiment N-23) and 336 hours of S-35 (Experiment N-25).

336 hours (N-25). Clearly the response time decreases with storm age. This strongly suggests that seeding operations are more likely to be successful with older storms. As we shall shortly see, the static stability of the eyewall region is increasing over the time span of the calculation. This further suggests that the changes of success in a seeding operation are greater the greater the static stability of the eyewall region.

The response times of the experiments which begin at 312 and 336 hours (N-23 and N-25) are comparable to those previously obtained (fig. 23). The experiment (N-22) which begins at 264 hours never shows MSLW less than that of the control. However, the curve indicates that a decrease in intensity would likely have occurred if the seeding had been extended over a longer period of time. This is verified by figure 25 which shows the result of an additional eight hours of seeding.

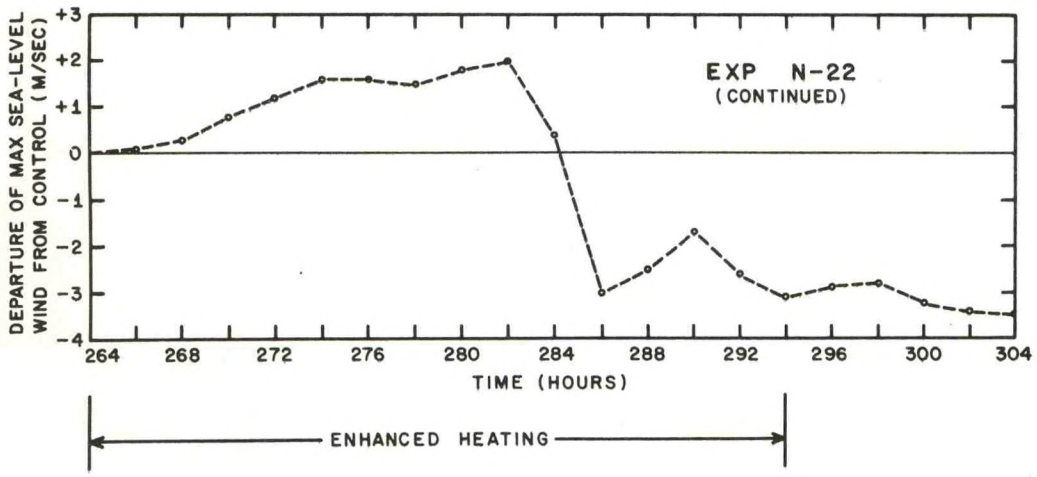

Figure 25. Same as experiment N-22 of figure 24 except that the seeding is continued for a total of 30 hours (264 to 294 hours).

Figure 26 is a time-cross section of temperature departures from values at 240 hours at the eyewall center (25-km radius) of the control (S-35). The warming is clearly concentrated in the upper troposphere and thus distributed such that static stability is increasing with time. Figure 27 shows the time dependence of precipitation at radii of 25, 35 and 45 km. In the eyewall, precipitation is decreasing by natural processes as the storm ages. At the two larger radii shown, natural processes are tending to increase the precipitation.

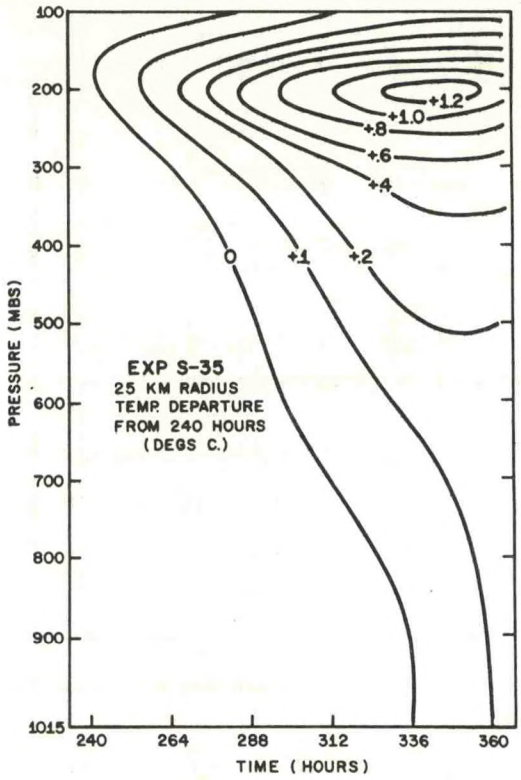

Figure 26. Time-cross section of temperature departures from their values at 240 hours at a radius of 25 km for experiment S-35.

Intuitively, increasing static stability of the eyewall, decreasing eyewall rainfall, and lateral spreading of the rain area would all seem to favor a seeding operation under the tactics of Hypothesis II.

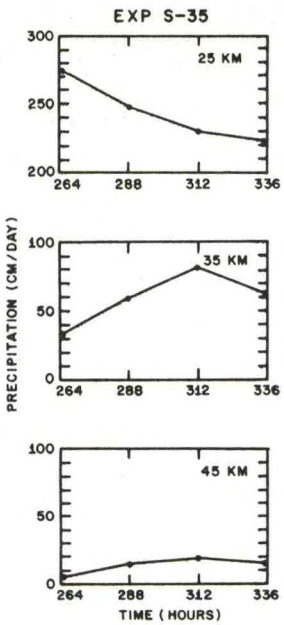

Figure 27. Rainfall rates as a function of time for selected radii for experiment S-35.

8. SUMMARY AND CONCLUSIONS

While only a small number of experiments are described here, consistent features emerge that, taken together with previous results (Rosenthal, 1971a), appear to allow certain generalizations. Clearly neither these calculations nor those of Rosenthal (1971a) provide support for Hypothesis I. It is our feeling that this strategy should not be employed in future field experiments.

The calculations indicate that of the potential tactics under Hypothesis II, a seeding operation just radially outward from the eyewall center is optimum. This is primarily reflected in the rapidity of response to the artificial heating rather than in ultimate reductions of the maximum winds. The latter were more or less the same for all calculations which succeeded in building a new eyewall at a larger radius. The experiments in which the artificial heating was applied at fairly large radii (beyond, say, 55 km) are probably pushing a point since in real hurricanes seedable clouds may be rather scarce in these locations. Despite this, the response times (all other factors being equal) were clearly greater with heating from the eyewall center outward and with heating at relatively large radii. The latter result may well reflect opposition to ascent due to the boundary layer "sucking" phenomenon discussed in Section 3.

The experiments clearly indicate that seeding must be continued until a new eyewall is formed at a larger radius if significant reductions of the maximum winds at sea level are to be achieved. On the other hand,

continued seeding, at the same radii, beyond the time that the new eyewall is established does not appear to be desirable. Comparison of Experiment N-5 (fig. 11) with Experiment N-4F (fig. 20) seems to indicate that this tactic may well reduce the effect of the earlier seeding. In all probability, the upward trend of the peak winds near the end of Experiments N-4D, N-23 and N-25 (fig. 24) represent this same effect.

In all successful calculations, the ultimate effect was to displace the eyewall 10 km (one grid point) radially outward from the original eyewall and to reduce the wind maximum at sea level by 3 to 4 m sec^{-1}. Variations in the radius of seeding and the rate of artificial heating altered only the time required for these changes to take place.

Response times decreased markedly with storm age. Intuitively, this appears to be related to an increase of the static stability of the control storm's eyewall as the model storm ages. In addition, aging of the control storm was accompanied by a natural tendency for eyewall rainfall to diminish and for rainfall to increase at radii just beyond the eyewall.

The increased transverse circulation which results from application of the artificial heating tends to increase winds at relatively large radii as inward transports of absolute angular momentum are increased. This is not a particularly desirable feature of a modification experiment since it may well produce adverse storm-surge effects. It also results in an increase of 20 percent in the modified storm's kinetic energy (Rosenthal, 1971a). On the other hand, we were able to show that these increased winds are vital if the eyewall is to be reformed at a larger radius and the maximum wind is to be reduced. It is the increased

centrifugal and coriolis forces arising from these larger winds that prevents the inflow from reaching the original eyewall and thus forces ascent at a larger radius.

While virtually all of the tactical variations of Hypothesis II ultimately resulted in similar modifications of the model hurricane, those with larger response times are clearly less likely to be effective in a real hurricane. It thus appears that field programs conducted with older storms, seeded just beyond the eyewall are most amenable to beneficial modification. It also appears that the seeding operation should be massive since larger heating rates clearly lead to more rapid responses of the model storm.

Since many of the numerical experiments show temporary increases of the maximum wind during the early phases of the operation, it would appear that the policy of not seeding storms whose early landfall is predicted should be continued.

9. ACKNOWLEDGMENTS

Members of the Advisory Panel of Project STORMFURY suggested several of these experiments. Frequent discussions with Drs. R. C. Gentry and H. F. Hawkins were of value in planning and interpreting the calculations.

REFERENCES

Anthes, R. A. (1971), Non-developing experiments with a three-level axisymmetric hurricane model, NOAA Technical Memorandum ERLTM-NHRL, (In press).

Anthes, R. A., S. L. Rosenthal, and J. W. Trout (1971), Preliminary results from an asymmetric model of the tropical cyclone, Monthly Weather Review, (In press).

Cotton, W. R. (1970), A numerical simulation of precipitation development in supercooled cumuli, NSF Grant No. GA-13818, (Dept. Meteorol., Pennsylvania State Univ., University Park, Pennsylvania), 178 pp.

Estoque, M. A. (1971), A hurricane model for simulating cloud seeding, NOAA Grant No. E-22-47-68(G), (Division of Atmospheric Sciences, Rosenstiel School of Marine and Atmospheric Science, University of Miami, Coral Gables, Florida), 16 pp.

Gentry, R. C. (1969), Project STORMFURY, Bulletin of the American Meteorological Society, 50, No. 6, 404-409.

Gentry, R. C. (1970), Hurricane Debbie modification experiments, August 1969, Science, 168, No. 3930, Apr. 24, 473-475.

Gentry, R. C. and H. F. Hawkins (1971), A hypothesis for modification of hurricanes, Project STORMFURY Annual Report 1970, U. S. Department of Navy and U. S. Department of Commerce, Appendix B, B-1 - B-15.

Hawkins, H. F. (1971), Comparison of results of the hurricane Debbie (1969) modification experiments with those from Rosenthal's numerical model simulation experiments, Monthly Weather Review, 99, No. 5, 427-434.

Hawkins, H. F. and D. T. Rubsam (1968), Hurricane Hilda, 1964: II. Structure and budgets of the hurricane on October 1, 1964, Monthly Weather Review, 96, No. 9, 617-636.

Hebert, P. J. and C. L. Jordan (1959), Mean soundings for the Gulf of Mexico area, National Hurricane Research Project Report No. 30, U. S. Department of Commerce, National Hurricane Research Laboratory, Miami, Florida, 10 pp.

Kuo, H. L. (1965), On formation and intensification of tropical cyclones through latent heat release by cumulus convection, Journal of the Atmospheric Sciences, 22, No. 1, 40-63.

Malkus, J. S. (1960), Recent developments in studies of penetrative convection and an application to hurricane cumulonimbi towers, Cumulus Dynamics, Pergamon Press, New York, 65-84.

Matsuno, T. (1966), Numerical integrations of the primitive equations by a simulated backward difference method, Journal of the Meteorological Society of Japan, Ser. 2, 44, 76-84.

Members, Advisory Panel to Project STORMFURY (1971), Report on meeting of Project STORMFURY Advisory Panel, Miami, Florida, 29-30 September 1970, Project STORMFURY Annual Report 1970, U. S. Department of Navy and U. S. Department of Commerce, Appendix A, A-1 - A-4.

Miller, B. I., (1962), On the momentum and energy balance of hurricane Helene (1958), National Hurricane Research Project Report No. 53, U. S. Department of Commerce, National Hurricane Research Laboratory, Miami, Florida, 19 pp.

Ooyama, K. (1969), Numerical simulation of the life cycle of tropical cyclones, Journal of the Atmospheric Sciences, 26, No. 1, 3-40.

Riehl, H. and J. S. Malkus (1961), Some aspects of hurricane Daisy, 1958, Tellus, 13, No. 2, 181-213.

Roll, H. U. (1965), Physics of the Marine Atmosphere, Academic Press, New York & London, 426 pp.

Rosenthal, S. L. (1969), Numerical experiments with a multilevel primitive model designed to simulate the development of tropical cyclones: Experiment I, ESSA Technical Memorandum, ERLTM-NHRL 82, U. S. Department of Commerce, National Hurricane Research Laboratory, Miami, Florida, 36 pp.

Rosenthal, S. L. (1970a), A survey of experimental results obtained from a numerical model designed to simulate tropical cyclone development, ESSA Technical Memorandum, ERLTM-NHRL 88, U. S. Department of Commerce, National Hurricane Research Laboratory, Miami, Florida, 78 pp.

Rosenthal, S. L. (1970b), A circularly symmetric primitive equation model of tropical cyclone development containing an explicit water vapor cycle, Monthly Weather Review, 98, No. 9, 643-663.

Rosenthal, S. L. (1971a), A circularly symmetric primitive-equation model of tropical cyclones and its response to artificial enhancement of the convective heating functions, Monthly Weather Review, 99, No. 5, 414-426.

Rosenthal, S. L. (1971b), Hurricane modeling at the National Hurricane Research Laboratory (1970), Project STORMFURY Annual Report 1970, U. S. Department of Navy and U. S. Department of Commerce, Appendix C, C-1 - C-13.

Rosenthal, S. L. (1971c), The response of a tropical cyclone model to variations in boundary layer parameters, initial conditions, lateral boundary conditions and domain size, Monthly Weather Review, (In press).

Rosenthal, S. L. and W. J. Koss (1968), Linear analysis of a tropical cyclone model with increased vertical resolution, Monthly Weather Review, 96, No. 12, 858-866.

Senn, H. V. (1971), A summary of radar precipitation echo heights in hurricanes, Project STORMFURY Annual Report 1970, U. S. Department of Navy and U. S. Department of Commerce, Appendix K, K-1 - K-18.

Sheets, R. C. (1969), Preliminary analysis of cloud physics data collected in hurricane Gladys, 1968, Project STORMFURY Annual Report 1968, U. S. Department of Navy and U. S. Department of Commerce, Appendix D, D-1 - D-11.

Sheets, R. C. (1969), Computations of the seedability of clouds in a hurricane environment, Project STORMFURY Annual Report 1968, U. S. Department of Navy and U. S. Department of Commerce, Appendix E, E-1 - E-4.

Simpson, R. H., M. R. Ahrens, and R. D. Decker (1963), A cloud seeding experiment in hurricane Esther, National Hurricane Research Project Report No. 60, 30 pp.

Simpson, R. H. and J. S. Malkus (1964), Experiments in hurricane modification, Scientific American, 211, No. 6, 27-37.

Sundqvist, H. (1970), Numerical simulation of the development of tropical cyclones with a ten-level model. Part I, Tellus, 22, No. 4, 359-390.

Yamasaki, M. (1968), Detailed analysis of a tropical cyclone simulated with a 13-layer model, Papers in Meteorology and Geophysics, 19, No. 4, 559-585.

APPENDIX

Table A.1. Characteristic parameters of the seeding simulations

Exp. No.	Initial Conditions	Seeding Rate ($KJ\ Ton^{-1}\ sec^{-1}$)	Seeded Radii (km)	Duration of Seeding (hours)
N-4	288 hrs (S-35)	1	25, 35, 45	10
N-4D	Do.	Do.	Do.	20
N-4F	Do.	Do.	35, 45, 55	Do.
N-5	Do.	Do.	Do.	10
N-6	Do.	2	25, 35, 45	Do.
N-11	Do.	Do.	25	20
N-12	Do.	Do.	15, 25	Do.
N-13	Do.	1	45, 55, 65	Do.
N-15*	Do.	Do.	25, 35, 45	Do.
N-21	304 hrs (N-4D)	Do.	35, 45, 55	16
N-22	264 hrs (S-35)	Do.	25, 35, 45	20
N-23	312 hrs (S-35)	Do.	Do.	Do.
N-25	336 hrs (S-35)	Do.	Do.	Do.
N-27	288 hrs (S-35)	Do.	75, 85, 95	Do.
N-45	Do.	Do.	25, 35, 45	12
N-46	Do.	Do.	Do.	14

*Experiment N-15 is conducted with temporally constant values of the coriolis and centrifugal terms in the radial equation of motion.